Ind. J. Pharm. Edu. Res., 2024; 58(2):565-578.
https://www.ijper.org

Original Article

Green Synthesis and Characterization of Silver Nanoparticles from *Nerium indicum* and Investigation of Antioxidant and Anti-Cancerous Potential against Cervical Cancer Cell Line (HeLa)

Rutuja Kini[1], Rashmi Trivedi[1], Mohd Hasan Mujahid[1], Pratikshya Patra[1], S. A. Alharbi[2], F. D. Alshammari[3], M. M. Babikir Bealy[4], A. E. O. Elkhalifa[5], Samra Siddiqui[6], Tarun Kumar Upadhyay[1,*]

[1]Department of Biotechnology, Parul Institute of Applied Sciences and Research and Development Cell, Parul University, Vadodara, Gujarat, INDIA.
[2]Department of Clinical Laboratory Science, College of Applied Medical Sciences, Shaqra University, Al-Quwayiyah, SAUDI ARABIA.
[3]Department of Clinical Laboratory, College of Applied Medical Science, University of Hail, Hail, SAUDI ARABIA.
[4]Department of Pathology, College of Medicine, University of Hail, Hail, SAUDI ARABIA.
[5]Department of Clinical Nutrition, College of Applied Medical Sciences, University of Hail, Hail, SAUDI ARABIA.
[6]Department Health Services Management, College of Public Health and Health Informatics, University of Hail, Hail, SAUDI ARABIA.

ABSTRACT

Background: Nanotechnology has introduced innovative approaches to clinical applications and drug delivery systems, and among the various nano-materials, AgNPs have garnered significant attention due to their biocompatibility, antibacterial properties, and versatile applications in the medical field. A major cause of cancer related death in women and the fourth most prevalent malignancy worldwide is the cervical cancer, posing a pressing global health challenge. **Materials and Methods:** In our study, we employed a green synthesis approach to produce AgNPs using leaf extracts from *NI* and assessed their potential for both antioxidant and anticancer applications against cervical cancer (HeLa) cells. Characterization of the AgNPs was conducted using various techniques, including zeta-sizer, UV-vis spectrophotometry, and FTIR analysis. **Results:** The UV-Vis spectroscopy results revealed peak value between 400-500 nm, affirming the successful synthesis of the nanoparticles. These AgNPs exhibited an average particle size of 300.4 nm with a PDI value of 0.610. Scanning Electron Microscopy (SEM) image reveal that synthesized nanoparticles are spherical in morphology. Further, assessing the anticancer potential of the *NI* AgNPs, the MTT assay revealed an IC_{50} value of 165 µg/mL, indicative of their effective anticancer activity against cervical cancer cells. Haemolytic inhibition assay showed that at lower doses particles has more haemolytic inhibition potential. Furthermore, we evaluated their impact on cancer cells by examining ROS generation, nuclear morphology with Hoechst staining, and apoptosis of HeLa cells with PI staining. Additionally, we assessed mitochondrial and acidic organelles' activity using MitoTracker and LysoTracker staining. Cell migration assay validated the inhibitory potential of *NI* AgNPs on the growth and migration of the cells. **Conclusion:** Our findings demonstrate that *NI* AgNPs possess notable potential as efficient anticancer agents against cervical cancer. This research underscores the promising role of green-synthesized AgNPs in the fight against cervical cancer and highlights their potential as a novel therapeutic strategy.

Keywords: Cytotoxicity, *Nerium indicum*, Silver nanoparticles, Cervical cancer, Haemolysis, Cell migration.

Correspondence:
Dr. Tarun Kumar Upadhyay
Department of Biotechnology, Parul Institute of Applied Sciences and Research and Development Cell, Parul University, Vadodara-391760, Gujarat, INDIA.
Email: tarun_bioinfo@yahoo.co.in

Received: 15-09-2023;
Revised: 09-11-2023;
Accepted: 15-01-2024.

INTRODUCTION

Nanotechnology is a significant branch of modern science that is engaged with the creation, organization, and structural modification of particles having sizes between 1 and 100 nm. A brand-new multidisciplinary field called nanotechnology combines knowledge from various fields, including medicine, pharmacology chemistry, material science, physics, engineering, and biology.[1] There are many types of NPs, in particular, inorganic nanoparticles are easily accessible, functional, compatible, and capable of drug targeting and controlled release. These characteristics make it suitable for cell delivery.[2] The potential of various antioxidant, antibacterial, anticancer properties and low toxicity to human cells of plant derived nanoparticles have made them widely used in medical imaging, therapeutic compounds,

DOI: 10.5530/ijper.58.2.63

food preservation, protective clothing, disinfectants, water treatment, viable germ-killing, wound dressings, cosmetics, disinfectants and for many more purposes.[3] According to the recent published literature review, many infectious species can be treated using silver nanoparticles including, *Pseudomonas aeruginosa, Staphylococcus aureus, E. coli, Vibrio cholera, Bacillus subtilis,* and *Syphilis typhus.*[4] Moreover, these silver nanoparticles are effective in the detection and therapy of cancer.[5]

In general, the production of nanoparticles involves several expensive and potentially environmentally hazardous chemical and physical processes that also require the use of poisonous and dangerous substances that pose various biological risks. Several accepted methods have been utilized for the preparation of nanoparticles.[6] It is crucial to ascertain whether these methods are risk-free, cost-effective, time-efficient, and environmentally friendly before therapeutic use. Numerous plant parts, including the stem, flowers, fruit, callus, peel, seeds, leaves, and roots, are used for the production of metallic nanoparticles of different sizes and shapes in biological systems. According to various studies, silver nanoparticles made using a green method have been used in both biomedicine and the management of pathogenic microbes. Cancer is one of the a life-threatening illness and biggest causes of mortality in the world.[7] According to the WHO, the number of cancer cases per year is expected to rise during the following two decades, from 14 million in 2012 to 22 million.[8] It explains how disease arises from unregulated cell growth and division driven by cellular changes that can result into malignant or benign tumor.

Cervical cancer cells HeLa is a malignant cell line from a strain that has been consistently growing since its isolation from a patient with cervical carcinoma in 1951. Cervical cancer is one of the leading causes of mortality due to cancer among women and the fourth most prevalent malignancy overall. Around 56,9847 new cervical cancer cases were diagnosed in 2018, and up to 31, 1365 fatalities from this cancer were reported globally.[9] The root cause for the spread of cervical cancer is the Human Papillomavirus (HPV). Treatment options for the cancer stage include surgery, radiation therapy, and chemotherapy. These treatment options have various side effects of the body thereby to get some therapeutics with no or minimum side effects, researchers are working towards some biological options such as green synthesis of nanoparticles that can be used as the alternate treatment options for the cervical cancer. In the present study, we have tried to examine the antioxidant and anticancer potential of the AgNPs synthesized from *NI* leaves on the cervical cancer cells.

MATERIALS AND METHODS

Silver nitrate, DPPH reagent (Himedia), MTT, DCFDA, Hoechst, LysoTracker, MitoTracker, and Propidium iodide dye (Invitrogen), DMSO (Sigma), Methanol (SDFCL), Ascorbic acid (Sulab), Trypsin EDTA solution (Himedia), DMEM (Himedia), Antibiotic and Antimycotic solution, FBS (Himedia), Trypan blue (Himedia).

Procurement and maintenance of cell line

HeLa cell line was procured from the NCCS Pune and cells were maintained at 37°C in a CO_2 incubator in DMEM 1640 (Gibco, No. 51800-019) media with FBS and Antibiotic and Antimycotic solution (Gibco) (10% and 1% respectively).

Preparation of Silver nanoparticles

Plant samples were collected from medicinal plant garden of Parul university, Vadodara, Gujarat, India. The leaves were properly washed with double distilled water to clean any undesirable debris before being dried for two days in a hot air oven. After being dried in the shade for a week, the *NI* leaves were ground into a fine, gritty powder. 10 g of the grounded powder was further mixed with 100 mL of double distilled water and stirred continuously for 20 min at 60°C. Further, mixture was allowed to cool till room temperature, filtered through Whatman No. 42 filter paper, and centrifuged for 20 min at 2000 rpm.[10] Prepared extract was collected and used for the synthesis of the Silver Nanoparticles (AgNPs). For the synthesis of AgNPs, 90 mL of a 1 mM aqueous solution of Silver Nitrate ($AgNO_3$) was mixed with 10 mL of the *NI* extract. This mixture was then kept in the dark at room temperature. The synthesized brown colour AgNPs were collected by centrifugation and air dried.[11]

UV-visible spectroscopy

This is one of the widely used methods for the characterization of particles. A UV spectrum was recorded between 200 to 700 nm to get the peak value for the AgNPs to confirm if the prepared particles were AgNPs.[12]

FTIR (Fourier transform infrared) analysis

Basis of the FTIR Spectroscopy method is the interaction between a sample and infra-red radiation. It determines the sample's absorption/transmission frequencies as well as the strength of these frequencies. The absorption of radiation at distinct frequencies is attributed to different chemical functional groups, making these frequencies valuable for identifying the chemical composition of a sample. FTIR spectroscopy was used to qualitatively validate the surface groups of the nanoparticles.[13] and a spectrum was recorded with a Bruker alpha FTIR spectrophotometer.

Size analysis

Size analysis of the prepared *NI* particles was performed with the Malvern Zeta sizer. The zeta sizer employs dynamic light scattering to determine particle size. This instrument utilizes illuminate the particles with the help of laser light and examines the variations in the intensity of scattered light. It assesses Brownian motion quantitatively and establishes a correlation with particle size.[14]

SEM analysis

SEM analysis of the prepared *NI* AgNPs was performed to determine the clear morphology of the particles.

Antioxidant assay (DPPH)

Antioxidants are essential nutraceuticals due to their diverse health benefits.[15] 1,1-diphenyl-2-picryl-hydrazyl (DPPH) is a well-known free radical which shows transitions from purple to yellow upon scavenging. We have performed the DPPH scavenging assay as per to the previously used protocol with some modifications.[16] DPPH solution (0.1 mM) was made by solubilizing DPPH in methanol resulting in a purple color solution. 20-100 µg/mL concentrations of the AgNPs were prepared using distilled water and mixed with 1 mL of 0.1 mM DPPH, and incubated for 30 min at room temperature in the dark and after incubation, absorbance was measured at 517 nm and ascorbic acid was taken as the standard. % radical scavenging activity of the DPPH was calculated by the given formula:

$$\%RSA = \frac{\text{Absorbance of control} - \text{Absorbance of sample}}{\text{Absorbance of control}} x100$$

Haemolytic activity

Haemolytic activity determination was performed according to the previously used protocol with some modifications.[17] Briefly, 5 mL of the blood was centrifuged, RBC pellet collected after supernatant was discarded and washed twice with PBS. 2 % of the RBC suspension was made in 1% NaCl and 1 mL of this suspension and 1 mL of 25, 50, 100, and 200 µg/mL of the *NI* AgNPs (dissolved in PBS) were mixed together. Mixture was the left for incubation in the dark at room temperature for 30 min and absorbance was measured at 540 nm. 1% Triton-100x was taken as positive control and PBS as negative control. % haemolytic inhibition was calculated with the help of given formula:

$$\%\text{ hemolytic inhibition} = \frac{\text{Absorbance of sample} - \text{Absorbance of negative control}}{\text{Absorbance of positive control} - \text{Absorbance of negative control}} x100$$

Anticancerous activity determination

Cytotoxicity assessment (MTT assay)

For testing the HeLa cells's viability, we have followed the previously described protocol.[18] 1×10^4 cells/well were seeded in 96-well plate of in 100 µL complete DMEM media. 96-well plate then incubated for 24 hr at 37°C in the incubator and then treated with 25 to 200 µg/mL of the *NI* AgNPs. After incubation, 10 µL of MTT (5 mg/mL) was added per well and further incubated for 4 hr, formazan crystals were visualised with FLoid imaging system and dissolved in 100 µL Dimethyl Sulfoxide (DMSO) per well after the supernatant was discarded. In order to completely dissolve the crystals, the plate was incubated for another 15 min, and the absorbance of the solution was analyzed with SynergyH1 ELISA plate reader at 570 nm. The % viability was calculated according to the given formula:

$$\%\text{Viability} = \left(\frac{\text{Absorbance of treatment}}{\text{Absorbance of control}}\right) X100$$

Trypan blue exclusion method

For the determination of the cell viability through Trypan blue we have followed previously used protocol with some modifications. Briefly, 50,000 cells per well were seeded in a 24 well plate and after incubation treated with the 25, 50, 100, and 200 µg/mL of the *NI* AgNPs. After treatment period over, cells were harvested and counted with the help of haemocytometer. Cells with the blue color stain were considered dead while bright color cells were considered live.[19]

Reactive Oxygen Species (ROS) generation

The mitochondrial electron transport chain is the most common source of ROS and it plays a key role in many cellular signalling mechanisms. Overproduction of ROS has been associated with a number of diseases. The production of intracellular ROS was observed using DCFHDA dye using previously described protocol.[20] 5×10^4 cells/well were seeded in a 24 well plate and left overnight for incubation at 37°C. After incubation, treatment of the cells was done with different concentrations of AgNPs (25-200 µg/mL) and incubated for 24 hr at 37°C. Cells were rinsed with PBS at the end of treatment period, and 20 µL of DCFH-DA dye was added for 30 min at 37°C. Following incubation for 30 min, cells were once again rinsed with PBS, and FLoid Imaging microscope was used to capture the images.

Nuclear morphology examination by Hoechst staining

Normally, healthy cells possess spherical nuclei with evenly distribute genetic material, therefore nuclear condensation can be use to distinguish apoptotic cells from normal cells. Apoptotic or dying cells show condensed and fragmented nuclei.[21] To examine the nuclear changes after the treatment with AgNPs, a 24 well plate was seeded with (5×10^4) cells/well and kept in a CO_2 incubator at 37°C overnight to ensure optimal cell adhesion. After the overnight incubation, cells were then treated with various doses of AgNPs (25 to 200 µg/mL), and the plate was then incubated for 24 hr at 37°C. After 24 hr, cells were rinsed with PBS and 10 µL of the Hoechst was added for the 15 min. After washing with PBS, cells were imaged under FLoid Imaging microscope.

LysoTracker Red DND 99 staining

Lysosomes are involved in intracellular signalling, energy consumption, secretions, and plasma membrane repair in the preservation of cellular homeostasis. LysoTracker DND Red 99 is a hydrophobic weak base and a live fluorescent marker that accumulates exclusively in acidic extracellular compartments, primarily early endosomes, and lysosomes.[22] Due to the acidic pH of the lysosomes, LysoTracker Red becomes protonated upon

entrance and is therefore significantly trapped in lysosomes resulting in intense red fluorescence. To study the lysosomal activity after the treatment with AgNPs, the 24 well plate was seeded with 5×10^4 cells per well, and the plate was incubated for 24 hr to ensure cell adhesion. After incubation was over, cells were treated with 25, 50, 100, and 200 µg/mL concentrations of the *NI* AgNPs and plate was incubated for further 24 hr at 37°C. 20 µL of LysoTracker red was added to each well after 24 hr, and the plate was then incubated for an additional 15 to 30 min. Cells were rinsed with PBS after the incubation period and imaged under FLoid Imaging microscope.

MitoTracker Red staining

All eukaryotic cells have mitochondria, which are the most numerous organelles and perform a variety of cellular functions. To study the structure of the mitochondria after AgNPs treatment and to investigate the ability of AgNPs to induce apoptosis by rupturing the mitochondrial membrane we have followed the previously described protocol for the mitochondrial staining.[23] $5x10^4$ cells/well were seeded into the 24 well plate and left for overnight incubationto ensure adequate cell attachment. After incubation, cells were treated with 25 to 200 µg/mL concentrations of *NI* AgNPs. The Plate was again incubated for 24 hr and after incubation, 20 µL of the MitoTracker dye was added and further incubated for 30 min. Cells were then washed with PBS and the plate was imaged under FLoid Imaging microscope.

Apoptosis determination through Propidium iodide staining

Propidium Iodide (PI) is a widely used red-fluorescent dye that doesn't stain live or early apoptotic cells because of the intactness of their plasma membrane. To determine apoptosis of the cells we have used previously described protocol with some modifications.[24] HeLa cells ($5x10^4$ cells/well) were seeded in a 24 well plate and incubated overnight. After incubation period over, cells were treated with 25 to 200 µg/mL of the *NI* AgNPs and incubated once again for 24 hr. After 24 hr, 20 µL of the PI was added in each well and again incubated for 15 min at 37°C. After washing with PBS, cells were imaged under FLoid Imaging microscope.

Hoechst and PI dual staining

Hoechst and PI dual staining was performed for the study of apoptosis and nuclear examination simultaneously. We have used the same protocol that we used of the separate Hoechst and PI staining and combined the filters used for the imaging. For the study, HeLa cells were cultured in DMEM medium for 24 hr, after the incubation, the cells were treated with various concentrations of *NI* AgNPs (25-200µg/mL) and incubated for the 24 hr period. After 24 hr, cells were rinsed with PBS, then after the cells were treated with 10 µL Hoechst and 10 µL PI dye and incubated for 15 min. Cells were again rinsed with PBS, and then observed under a FLoid imaging microscope.

LDH Release determination

LDH release determination was performed using CyQUANT™ LDH Cytotoxicity Assay Kit and protocols used as per the manufacturers' instructions. In brief, $5x10^4$ cells/well seeded in a 24 well plate and left overnight for incubation. After attachment and growth of the cells, treatment with *NI* AgNPs (25-200µg/mL) was performed and again incubated for 24 hr. After incubation, 10 µL of 10X Lysis Buffer was added in the maximum LDH toxicity control wells and incubated for 45 min at 37°C. For the spontaneous release, 100 µL of sterile distilled water was added. After 45 min incubation, 50 µL/well supernatant was taken into a 96 well plate and 50 µL of Reaction Mixture was added to each sample well following 30 min room temperature incubation. Further, 50 µL of Stop Solution was added into each well, absorbance was taken within 1 to 2 hr at 490 nm and 680 nm. Next background absorbance value at 680 was subtracted from the 490. % cytotoxicity/LDH release was calculated with the help of give formula:

$$\%\ \text{LDH release} = \frac{\text{Compound treated LDH actvity} - \text{Spontaneous LDH activity}}{\text{Maximum LDH activity} - \text{Spontaneous LDH activity}} \times 100$$

Cell scratch assay

Cell scratch assay was used to measure the migration potential of cell in the treated as well as in the control wells. We have followed the previously published protocol.[25] In brief, 50,000 cells per well seeded in a 24 well plate and left until they got complete confluency. After that a scratch was made with the help of the 10 µL tip and cells were washed with the PBS. Cells were treated with the 25 to 200 µg/mL of the *NI* AgNPs and left for 24 hr incubation. After incubation and washing with PBS, cells were again imaged under the inverted microscope to get the migration area of the cells.

Statistical analysis

All the experiments were performed in triplicate and GraphPad Prism and One way ANOVA were used for the statistical analysis. All the values below p 0.05 ($p<0.05$) were considered significant. ***is used for highly significant, **for less significant, *for least significant and ns for the non-significant values.

RESULTS

Preparation of Silver nanoparticles

1:9 ratio of the leaf extract and 1 mM aqueous solution of Silver Nitrate ($AgNO_3$) was mixed and resulted in the color change from white to dark brown indicating the formation of AgNPs as shown in Figure 1.

UV-visible spectroscopy

Dark brown-coloured prepared particles were characterized with the UV-vis spectroscopy to confirm the preparation of *NI* AgNPs. AgNPs have their specific characterization peak between 400-500 nm.[24] We have taken 20-100 µg/mL of the concentrations of the prepared particle and spectra was recorded between 300-700 nm. We have found the peak value between 400-500 nm confirming that the prepared partilces are *NI* AgNPs as shown in Figure 2.

FTIR (Fourier Transform Infrared)

The FTIR spectra of *NI* AgNPs was recorded between 600 to 3600 cm^{-1} as shown in Figure 3. Transmittance peaks at 3,417.91 cm^{-1} is indicating the presence of OH functional group and C=O functional groups were presented at 3249.92 cm^{-1}. Peaks at 1498.39 cm^{-1} has a C=C functional group and with the vibration type of Stretch, while the peak at 1356.35 cm^{-1} is showing the C–N stretching of the aromatic amine group and stretching vibrations at 639.24 cm^{-1}.[26] A spectrum having almost similar type of peak patterns was reported in our study confirming that prepared particles are *NI* AgNPs.

Zeta sizer analysis

The Zeta sizer allows users to analyze the particle size and Polydispersity Index (PDI) of the particles. Particle size and distribution of the *NI* AgNPs are shown in Figure 4. Particles have an average size of 300.4 nm and a PDI value of 0.610. PDI value under 1 is indicative of the homogenous nature of the particles.

SEM analysis

SEM analysis of the prepared particles at the 400 nm resolution showed that particles are spherical in nature as shown in Figure 5.

DPPH (Free Radical Scavenging Activity)

Efficient radical scavenging activity was observed with the *NI* AgNPs. % RSA was found to increase as the concentration increased from 20 to 100 µg/mL and Maximum % RSA was found at 100 µg/mL as shown in Figure 6a.

NI AgNPs showed dose dependent decrease of % haemolytic inhibition

Haemolytic inhibition is the assay that defines the blood compatibility of the compound. In our study, we have reported that at the 25 µg/mL of the concentration *NI* AgNPs were able to inhibit almost 66% of the haemolysis while at the highest concentration i.e. 200 µg/mL, this % haemolytic inhibition decreased up to 37% as shown in the Figure 6b.

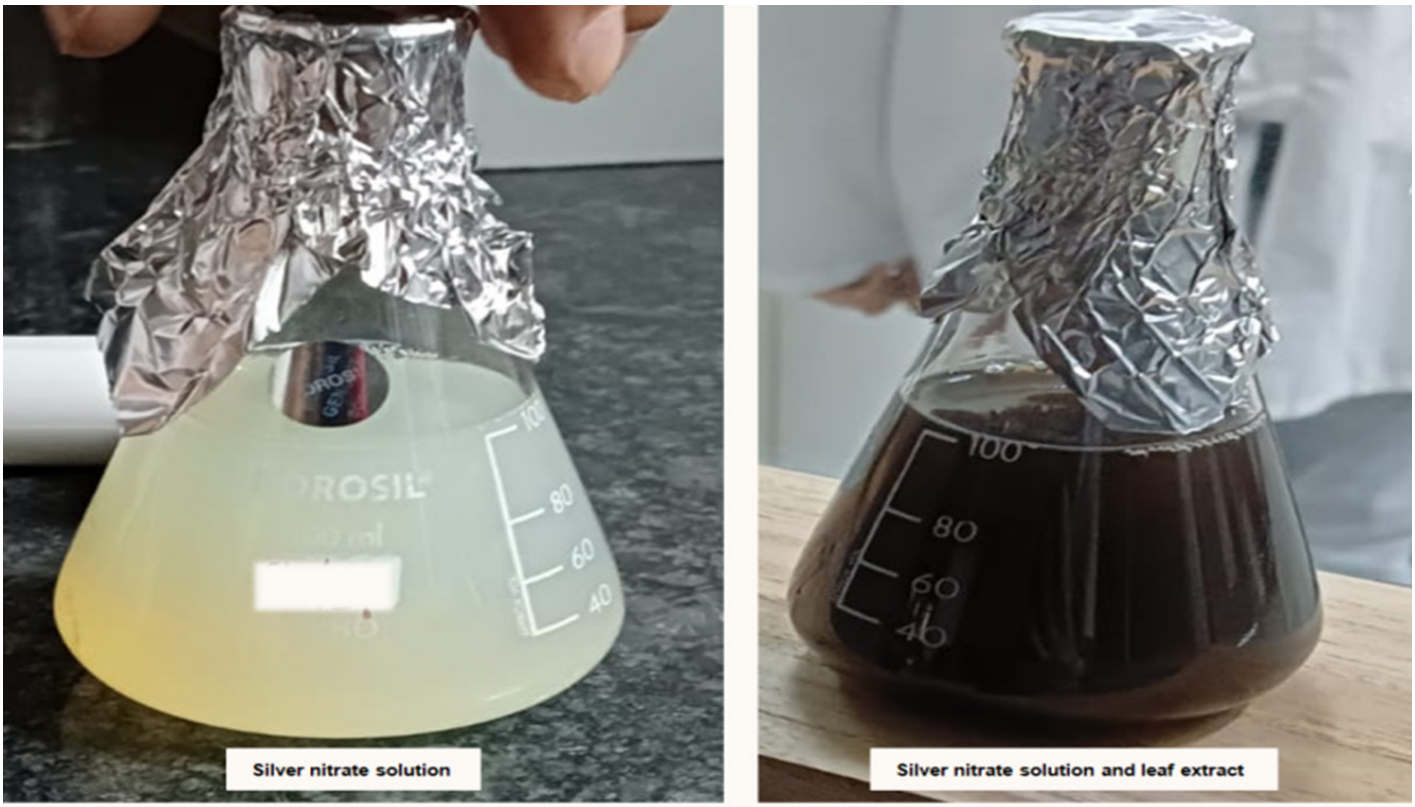

Figure 1: White color silver nitrate solution resulted in to formation of dark brown color of *NI* AgNPs.

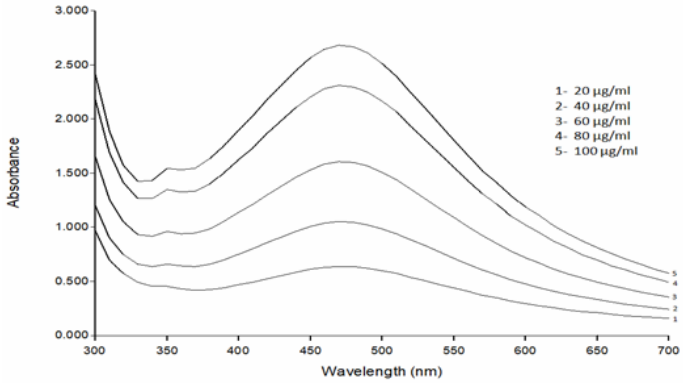

Figure 2: Absorbance spectra of the *NI* AgNPs recorded between 300-700 nm showing the peak value in the range of 400-500 nm.

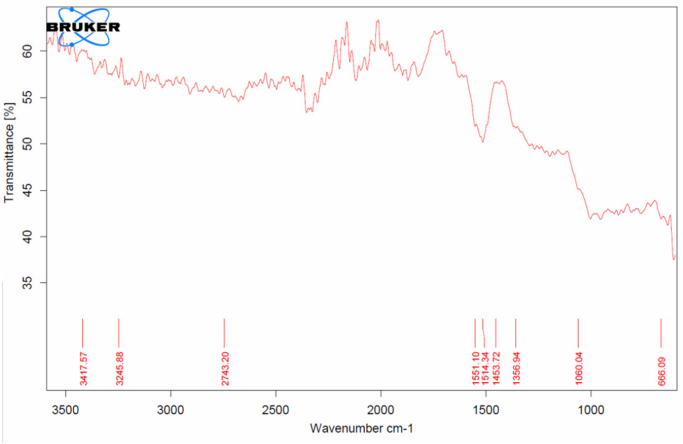

Figure 3: FTIR transmittance spectra of the *NI* AgNPs showing the major peaks at a wave number of 666, 1060, 1356, 1453, 1551, 2743, 3245, and 3417 cm^{-1} as per the reported studies.

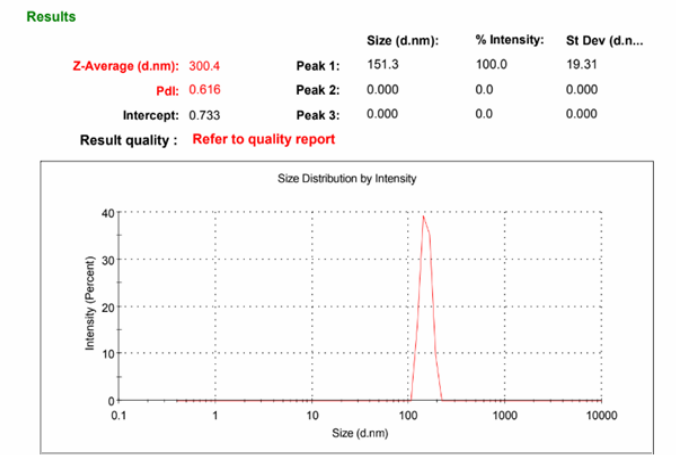

Figure 4: Size analysis of the particles showing average diameter of 300.4 nm and PDI value of 0.6 indicating the uniform distribution of the particles.

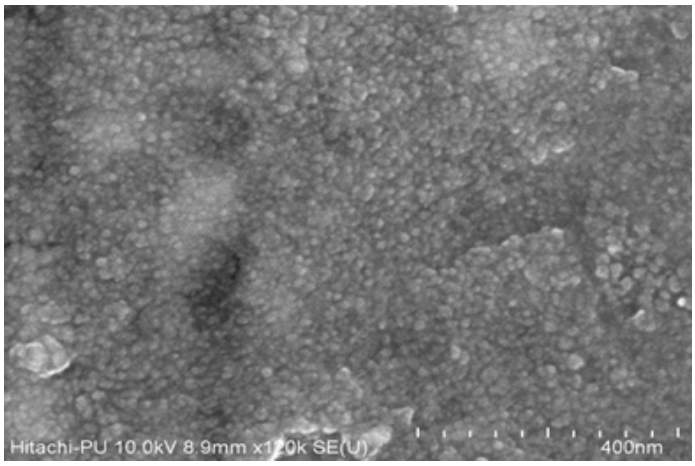

Figure 5: SEM image of synthesized *NI* AgNPs from *Nerium indicum.*

Results of anticancer activity

Cytotoxic effect (MTT assay)

Cytotoxic effect of the *NI* AgNPs was determined with the help of MTT assay. With the increase in treatment concentration, cell viability was decreasing and IC_{50} was found at 165 µg/mL as can be seen in Figure 7a. Maximum cytotoxicity was at 200 µg/mL concentration in comparison with control.

Trypan blue exclusion assay showed dose dependent decrease in cell viability

Trypan blue dye is exclusive for the dying cells. Although if incubation period is very long, healthy cells also start to take the stain so we have counted the cells with the help of the haemocytometer within 5 min after adding the Trypan blue in the cell suspension. Here we have reported a in the cell viability of HeLa cells with the increase in concentration as shown in the Figure 7 (b).

ROS generation was found to increase in a dose dependent manner

ROS generation is the normal process of the cells and it is required for the various cellular activities. ROS generation is controlled by various mitochondrial enzymes and it remains in a maintained state. If because of any reason, this ROS generation exceeds its limits, it causes damage to the cells. In our experiment, we have found a dose dependent increase in the intracellular ROS generation that is indication of the apoptosis of the cells as shown in Figure 8.

Hoechst staining confirmed the nuclear morphological changes

Hoechst dye is specific for the interaction with the nucleus of the cell. It is a DNA binding dye and gives blue color of the fluorescence upon binding with DNA. Any deformalities in the DNA can be easily visualised with this dye. In our experiment, we have found that in the control wells, nucleuses have uniform

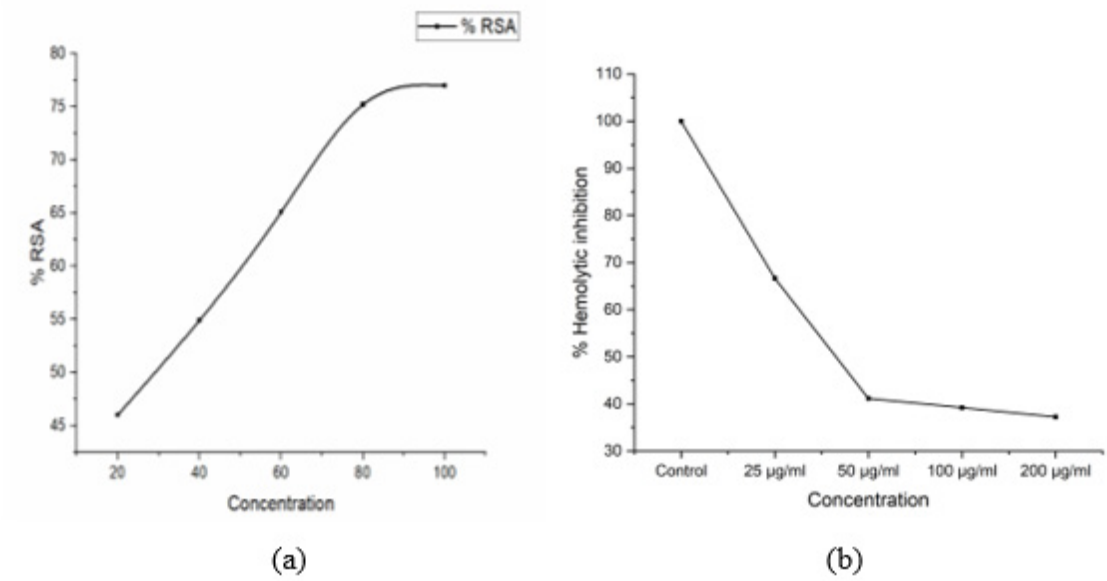

Figure 6: (a) Dose dependent increase in % RSA indicating efficient antioxidant activity of *NI* AgNPs. (b) Haemolytic inhibition was found to decrease in a dose dependent manner of *NI* AgNPs.

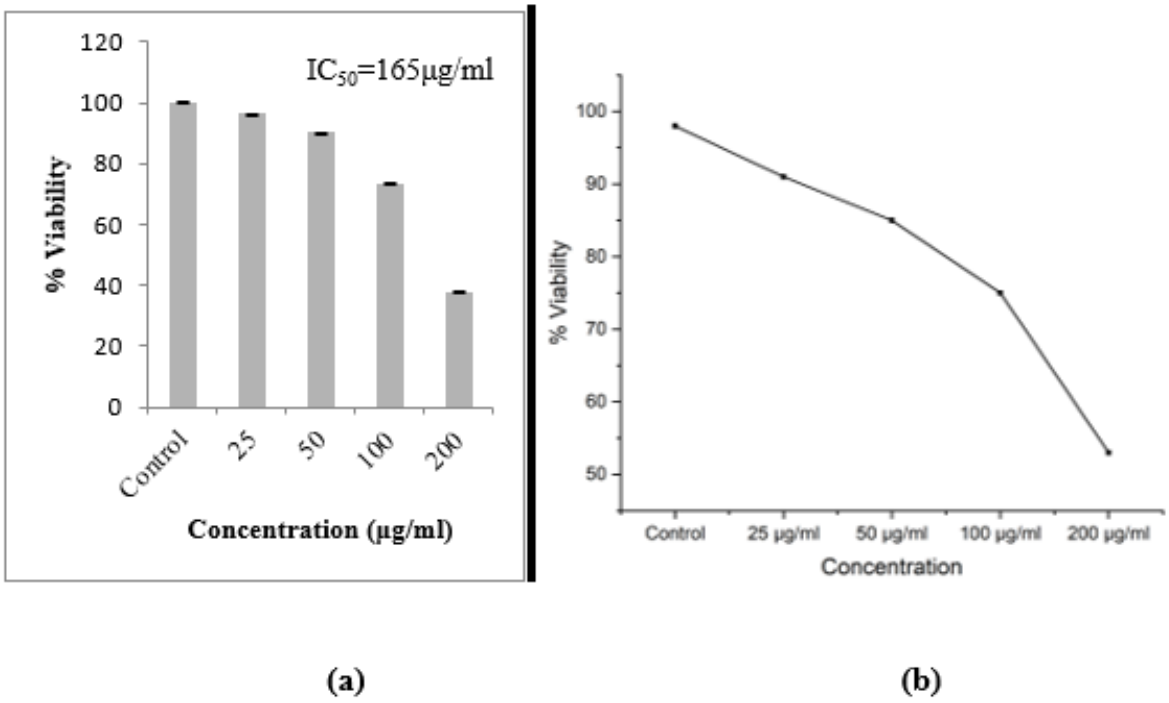

Figure 7: (a) Cell viability determined by MTT assay. Control cells having 100% cell viability while it was decreased with increase in the concentration of the *NI* AgNPs dose. A clear dose-dependent cytotoxic effect was observed with increasing concentrations of *NI* AgNPs. (b) Trypan blue exclusion assay showing a decrease in the cell viability with the increase in concentration after the treatment with *NI* AgNPs.

round or spherical shape but the treatment wells nuclear morphology is somewhat lost. Deformities of the nucleus were in dose dependent manner as shown in Figure 9 indicating the efficient anticancer activity of the *NI* AgNPs and maximum nuclear changes were present at 200 µg/mL. Nuclear deformalities are indicated by yellow color arrow.

LysoTracker Red DND 99 staining showing pH alterations of the acidic organelles

LysoTracker dye is specific for the acidic organelles and it enters only in lysosomes of live cells because of their less pH.[27] Due to the alteration in pH of the lysosomes or acidic organelles, dye is not retained well in the cells resulting in the less or decreased

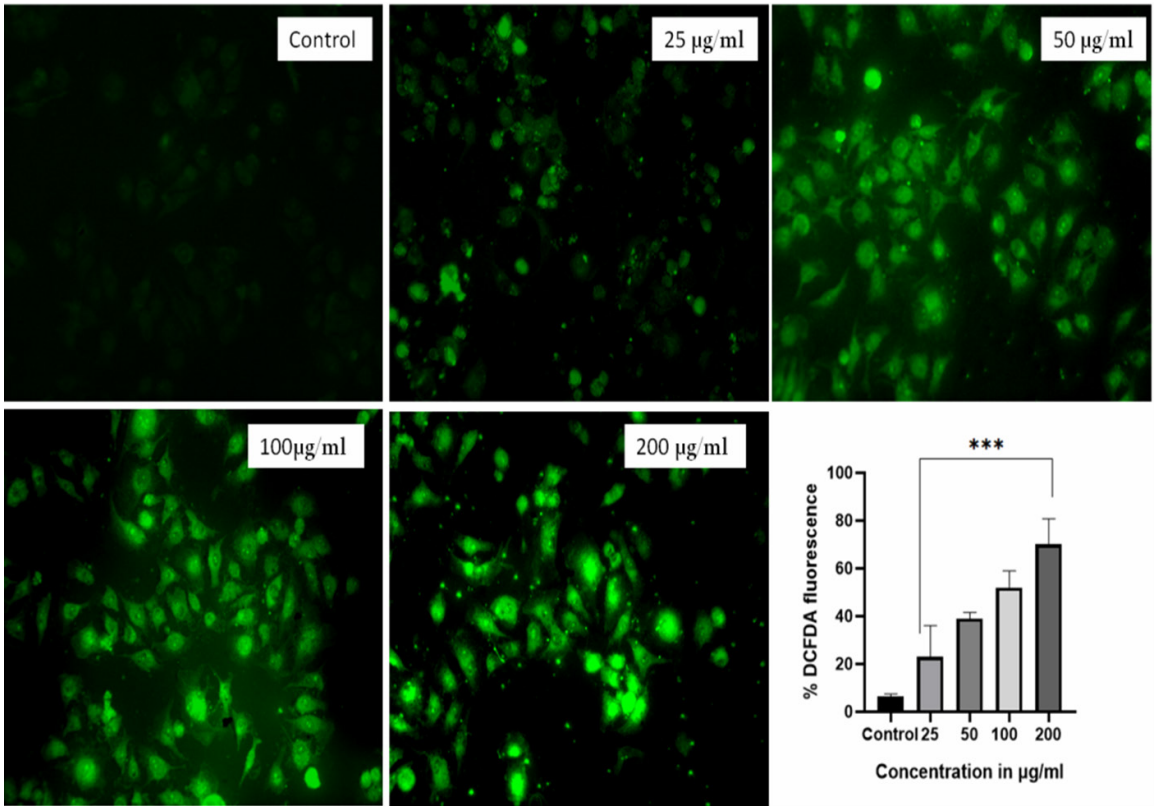

Figure 8: Generation of intracellular ROS leading to the damage to the cells. Maximum ROS generation was reported at 200 µg/mL concentration and statistical analysis of the results indicated all the values are highly significant with $p<0.05$.

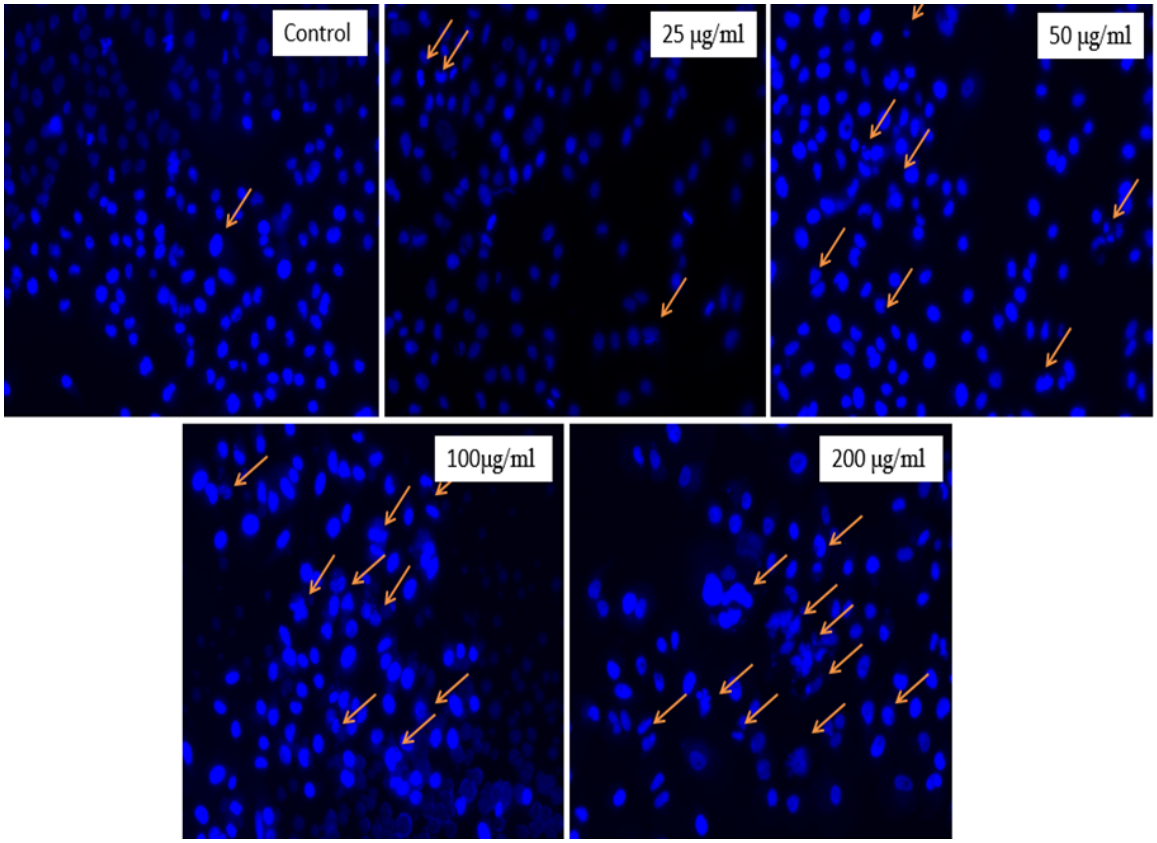

Figure 9: Morphological changes and nuclear fragmentation is increasing in the dose dependent manner. Maximum deformalities are present at 200 µg/mL concentration indicating that cells are undergoing apoptosis.

fluorescence intensity. In this study, the fluorescence intensity was found to decrease as increase in the AgNPs concentration as shown in the Figure 10.

MitoTracker Red CMX ROS indicating change in MMP

Both mitochondrial damage and an increase in MMP (mitochondrial membrane potential) have been linked to an increase in reactive oxygen species.[28] MitoTracker Red CMX ROS fluorescence is found to decrease in our study indicating a significant change in the MMP as shown in Figure 11.

Propidium iodide staining indicating apoptosis of HeLa cells

PI is an apoptosis indicating dye as it has the potential to enter into the dead or the cells undergoing apoptosis only. The results of our study indicating that *NI* AgNPs induced apoptosis in HeLa cells as the fluorescence intensity of the PI was found to increase in a dose dependent manner as shown in Figure 12.

Hoechst and PI dual staining

Hoechst and PI dual staining was performed to visualize the nuclear morphology and apoptosis together. Due to the use of both blue and red dye, the apoptotic cells were appeared as pink/red in color as shown in Figure 13a. We have found that nuclear morphological changes and apoptosis were increasing in a dose dependent manner.

LDH release

LDH (a soluble cytoplasmic enzyme) release in the cells is the indicative of the cell death and it can be used to validate MTT. LDH release in indicative of loss of cytoplasmic membrane integrity and this loss leads to the release of this enzyme in the cytoplasm. In our study, we have reported a dose dependent increase in the LDH release as shown in Figure 13 (b). This increase in LDH release indicates that LDH is being released into the cytoplasm and cells are undergoing apoptosis by the treatment of *NI* AgNPs.

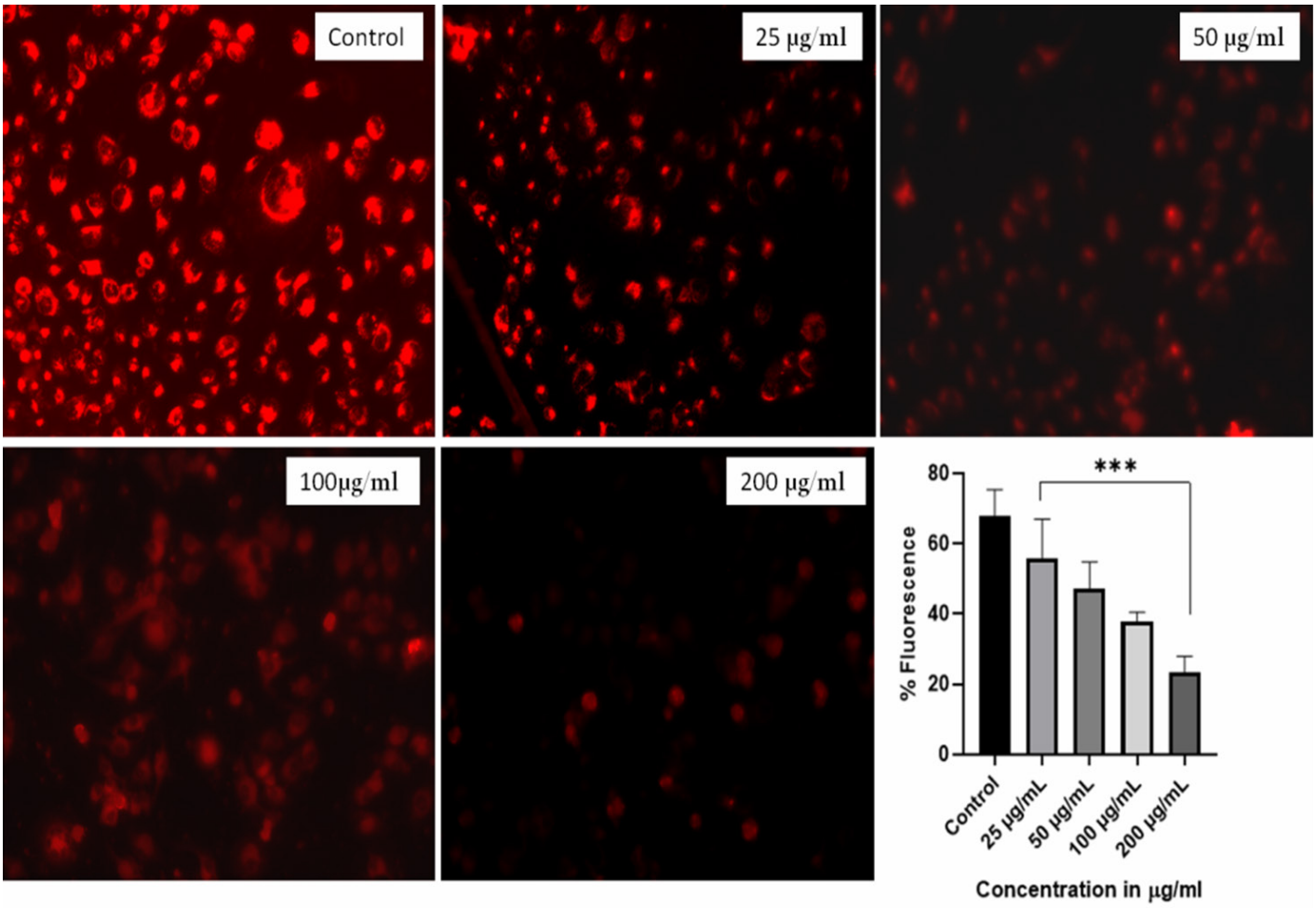

Figure 10: LysoTracker Red DND 99 staining showing the pH alteration of the acidic organelles. Statistical analysis showed that all the values were highly significant with respect to the control with a p value of less than 0.005 ($p<0.005$).

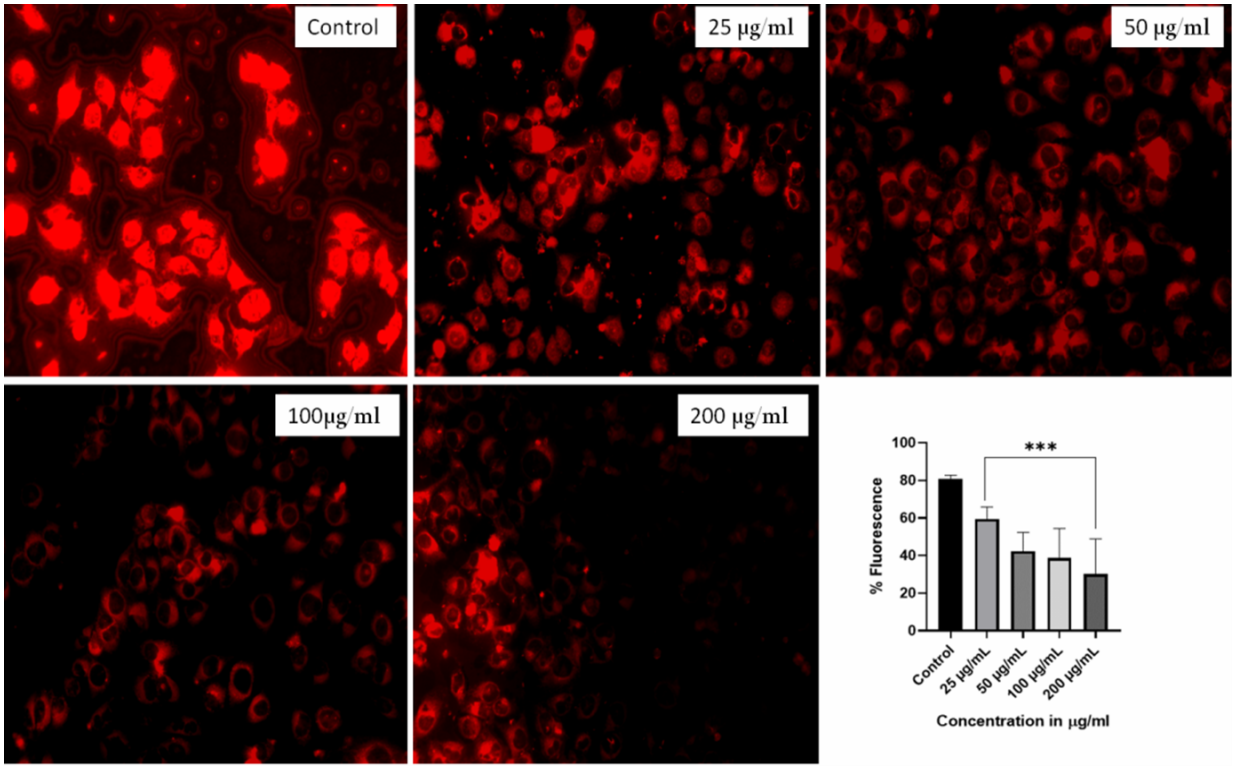

Figure 11: MitoTracker Red staining is showing the efficient change in the MMP due the treatment with *NI* AgNPs. Statistical analysis with one way ANOVA showed that all the values were highly significant with respect to the control with *p* value less than 0.005 (*p<0.005*).

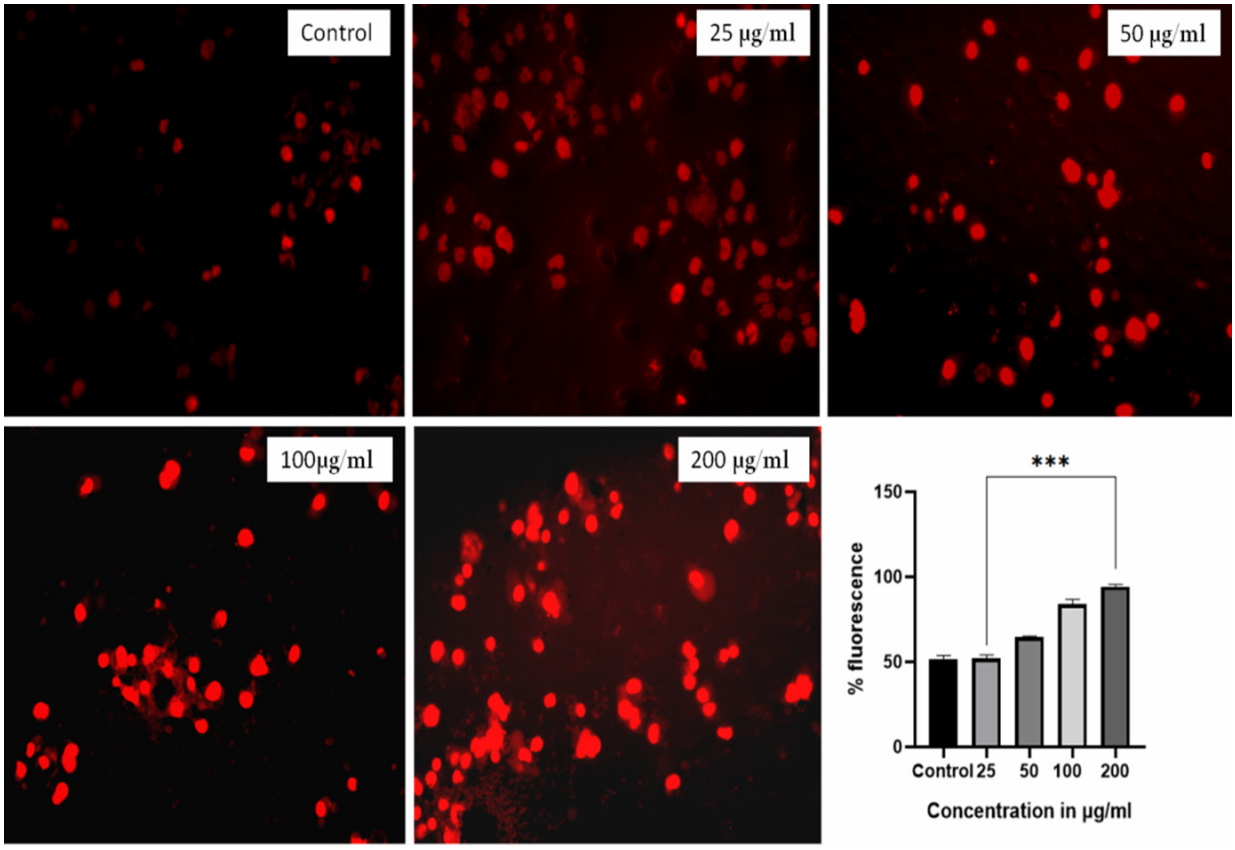

Figure 12: Propidium Iodide staining showing that *NI* AgNPs caused the HeLa cells to undergo apoptosis. The statistical analysis showed that all the values were highly significant with respect to the control with p value less than the 0.005 (*p<0.005*).

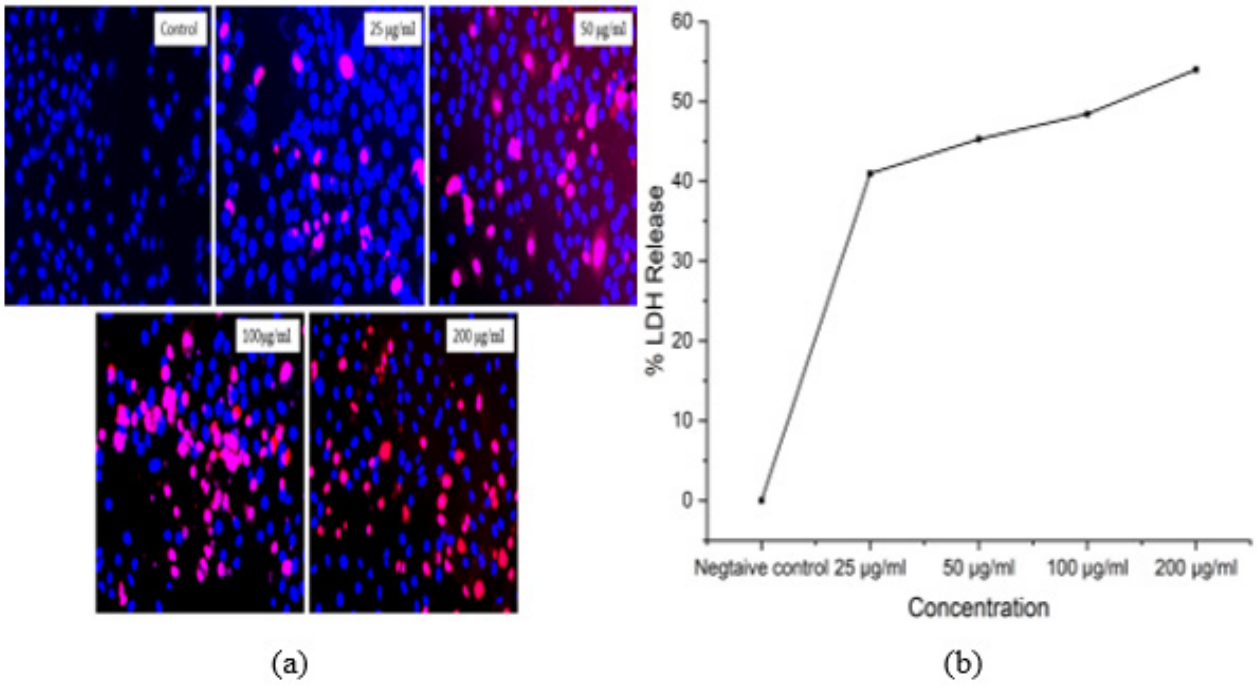

Figure 13: (a) In the Hoechst and PI dual staining, control cells were observed as blue color only indicating no apoptosis induction in control cells while the increase in pink color of fluorescence was showing that *NI* AgNPs are effective against cervical cancer and inducing apoptosis in HeLa cells. (b) LDH is normally present in all the cells and it gets released upon the rupture of plasma membrane. Here increasing % LDH release indicating that cells are having dose dependent apoptosis.

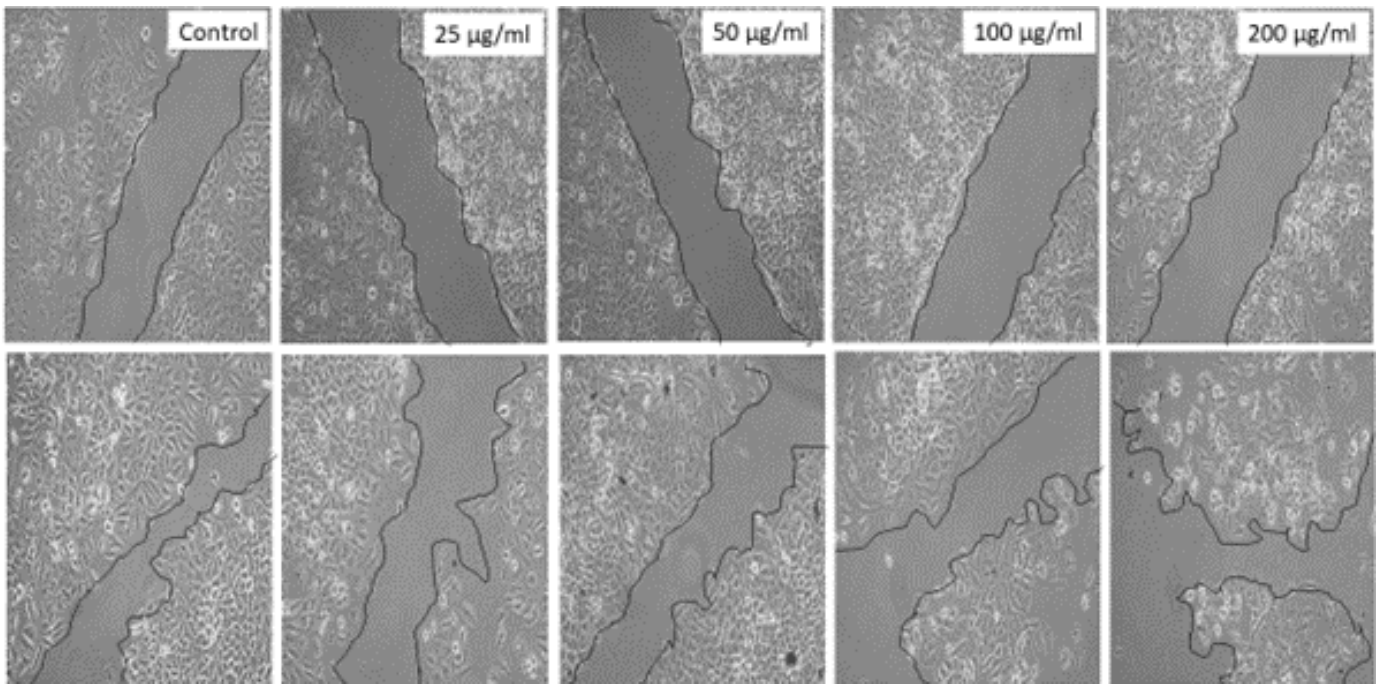

Figure 14: Cell scratch assay showing the increase of scratch area with the treatment while control cells covered most of the scratched are by cellular growth.

Cell scratch assay

In the cell scratch assay, we have reported that in the control wells cells have efficient normal growth and covered most of the growth area in the 24 hr. In the treated well, scratch area was increasing in a dose dependent manner and at the concentration of 200 µg/mL, most of the cell area was empty due to apoptosis of the cells as can be seen in Figure 14.

DISCUSSION

The development of novel medicinal compounds has been influenced by plants, and medications derived from plants have significantly contributed to human health. Various diseases can be treated with the help of phytomedicines. Plant-based medications offer tremendous therapeutic promise because they may accomplish the same goals as synthetic pharmaceuticals with no or less side effects.[29] The findings of our study suggested that *NI* AgNPs synthesized from leaf extracts can be used as naturally derived anticancer therapeutic. In our study, prepared particles firstly examined with UV vis spectroscopy that showed a valid peak as per the reported studies conforming that prepared particles are *NI* AgNPs.[30] The presence of the C-O stretch, OH stretch, CH-OH stretch, and C-H stretchand functional group of *NI* AgNPs were verified by FTIR analysis. Our recorded spectra were also demonstrating the resemblance with the spectra recorded by Subbaiya *et al.*, 2014 in which they have reported OH function groups at 3698.28cm^{-1} and 3403.05cm^{-1} and CH functional group at 2926.33cm^{-1}. C=C functional groups were reported at 1622.25 and 1500.39cm^{-1} respectively and NO functional groups were reported at 1500.39 cm^{-1}. CO group was present at 1216.78cm^{-1}.[12] Same kinds of peaks were reported in our study confirming the particle formation. PDI value of less than 1 in indicative of homogenity of the particles and we have found that our prepared particles were having a PDI 0.616 that is an indication of narrow size distribution of *NI* AgNPs.[31]

NI AgNPs were found to have an efficient DPPH free radical scavenging activity as reported in many studies. In research, *Nerium olender* flower extract synthesized AgNPs were reported to exhibit antioxidant activity and antimicrobial properties.[32] In our study, *NI* AgNPs were found to have strong antioxidant properties. % RSA was increasing in a dose dependent manner. Further, we have conducted the blood compatibility test to demonstrate the % haemolytic inhibition by the treatment of *NI* AgNPs. We have found that higher concentrations are having less potential to inhibit haemolysis of the RBCs. To assess cytotoxic potential, an MTT test was performed in which cell growth and survival was directly correlated with the rate of tetrazolium reduction. Cells internalize MTT, which is then reduced by mitochondrial enzymes and transferred to the cell's surface to create formazan crystals.[33] We have reported a dose dependent increase in cytotoxicity of the *NI* AgNPs. Same results were also obtained by research on the MCF-7 cell line of the breat cancer by the treatment with tungsten nanoparticles.[34] We have also performed the Trypan blue exclusion assay to determine the cell viability using the dye Trypan blue and we reported a dose dependent decrease in the cell viability of the HeLa cells. Hussein and Mohsin. 2019 also reported the same pattern of the cell viability by Trypan blue exclusion assay.[19] They also reported that if cells are kept in the Trypan blue for more than the 5 min, the live cells also start to take up the stain. Overproduction of ROS can harm mitochondrial complexes as well as enzymes.[35] To assess the reactive oxygen species generation, we have used DCFHDA dye. In our investigation, cells treated with *NI* AgNPs exhibited anticancer effects through the generation of ROS resulting in oxidative stress and cell death. It was found that ROS generation increased as the treatment concentration of *NI* AgNPs increased.

The hydrophobic dye known as Hoechst selectively attaches to the AT-rich regions of DNA in the minor groove and stains live/dead cells. Hoechst staining in our study showed that *NI* AgNPs have the potential to damage HeLa cells and that was observed through nuclear fragmentation and deformalities. LysoTracker red dye is specific for the acidic organelles and it bind to them due to their less pH. pH shift in the acidic organelles leads to less binding of the dye in the cells that ultimately results in reduced fluorescence intensity indicating cell death.[36] Moreover, MitoTracker Red CMX-ROS is a positively charged dye that gathers in the mitochondrial matrix owing to the negative MMP. This dye does not accumulate well in apoptotic cells due to the shift in MMP from negative to positive indicating apoptosis of the cells.[37] Saeed *et al.*, 2023 also reported a decrease in MMP in HeLa cells due to the treatment with zinc oxide nanoparticles.[38] In our findings, we reported the reduced fluorescence intensities of the LysoTracker and the MitoTracker dyes that was a clear indication of the apoptosis of the cells due to pH and MMP change. Khalil *et al.*, 2022 reported that $CaCO_2$ cells were showing a dose dependent increase in the LDH release when treated with the biosynthesized silver nanoparticles. The same pattern we have observed in our study.[39] Cell migration is a phenomenon that can measure the coordinated movement of the cells regulated by various factors such as cell-cell adhesion, polarization, cytoskeletal activity and mechanical and chemical cues. *In vitro* assays such as scratch assays allow us to quantify the migratory capacity of the cells under the controlled experimental conditions.[40] We have reported the migration of the HeLa cells in a higher rate in control than the treated cells. Bobadilla *et al.*, 2019.[40] also reported the same types of results in which control cells were able to cover almost whole well area by migration while treated wells are found to have less migratory capacity. In another study, HeLa cells treated with baicalein were also not able to migrate and the cell free area was increasing due to the effect of the treatment.[41] Overall, our study's results showed that *NI* AgNPs have the potential to reduce or inhibit the HeLa cells growth and proliferation.

CONCLUSION

In conclusion, our study has provided compelling evidence for the therapeutic potential of *NI* AgNPs synthesized from leaf extracts. These naturally derived nanoparticles have demonstrated promising characteristics that make them valuable candidates for various biomedical applications, particularly in the realm of cancer treatment. Our study mainly focused on the multifaceted anticancer potential of *NI* AgNPs, from their antioxidant properties to their ability to induce ROS generation, nuclear damage, and apoptotic pathways. Blood compatibility test is also a parameter in our study to evaluate the actual toxicity of the compound in the blood. These findings pave the way for further research and development of *NI* AgNPs as a promising and naturally derived therapeutic approach in the fight against cancer, offering the potential for reduced side effects compared to synthetic pharmaceuticals. Further *in vivo* studies and clinical investigations are warranted to fully explore the translational potential of these nanoparticles in cancer therapy.

ACKNOWLEDGEMENT

This research has been funded by the Scientific Research Deanship at the University of Ha'il, Saudi Arabia, through project number RG-20193.

FUNDING

This research has been funded by the Scientific Research Deanship at the University of Ha'il, Saudi Arabia, through project number RG-20193.

CONFLICT OF INTEREST

The authors declare that there is no conflict of interest.

ABBREVIATIONS

NI: *Nerium indicum*; **AgNPs:** Silver Nanoparticles; **ROS:** Reactive oxygen species; **HPV:** Human Papilloma Virus; **DMEM:** Dulbecco's Modified Eagle Medium; **FTIR:** Fourier transform infrared; **SEM:** Scanning Electron Microscopy; **DPPH:** diphenyl-2-picryl-hydrazyl; **DMSO:** Dimethyl sulfoxide; **PI:** Propidium iodide; **LDH:** Lactate Dehydrogenase.

SUMMARY

The study explored the therapeutic potential of naturally derived *NI* AgNPs synthesized from leaf extracts. Characterization techniques confirmed the nanoparticles' formation and highlighted their homogeneity and specific functional groups. *NI* AgNPs demonstrated strong antioxidant properties, efficient DPPH free radical scavenging, and dose-dependent cytotoxicity on cancer cells, evidenced by MTT and Trypan blue assays. Moreover, their impact on ROS generation, mitochondrial activity, and cell apoptosis was observed through various dye staining and fluorescence intensity assays. The study suggested that *NI* AgNPs could hinder cell growth and migration, showcasing their potential in inhibiting cancer cell proliferation.

REFERENCES

1. Moritz M, Geszke-Moritz M. The newest achievements in synthesis, immobilization, and practical applications of antibacterial nanoparticles. Chem Eng J. 2013; 228: 596-613. doi: 10.1016/j.cej.2013.05.046.
2. Xu ZP, Zeng QH, Lu GQ, Yu AB. Inorganic nanoparticles as carriers for efficient cellular delivery. Chem Eng Sci. 2006; 61(3): 1027-40. doi: 10.1016/j.ces.2005.06.019.
3. Habeeb Rahuman HB, Dhandapani R, Narayanan S, Palanivel V, Paramasivam R, Subbarayalu R, *et al.* Medicinal plants mediated the green synthesis of silver nanoparticles and their biomedical applications. IET Nanobiotechnology. 2022; 16(4): 115-44. doi: 10.1049/nbt2.12078, PMID 35426251.
4. Nel A, Xia T, Mädler L, Li N. Toxic potential of materials at the nanolevel. Science. 2006; 311(5761): 622-7. doi: 10.1126/science.1114397, PMID 16456071.
5. Popescu M, Velea A, Lőrinczi A. Biogenic production of nanoparticles. Dig. J. Nanomater. Biostruct. (DJNB). 2010; 5(4).
6. Vikas G, Payal M. Phytochemical and pharmacological potential of *Nerium indicum*: a review. Int J Pharm Sci Res (IJPSR). 2010; 1(3): 21-7.
7. Gao X, Lu Y, Fang L, Fang X, Xing Y, Gou S, *et al.* Synthesis and anticancer activity of some Novel 2-Phenazinamine derivatives. Eur J Med Chem. 2013; 69: 1-9. doi: 10.1016/j.ejmech.2013.07.017, PMID 23995213.
8. McGuire S. World cancer report 2014. Geneva, Switzerland: World Health Organization, International Agency for Research on Cancer, WHO Press, 2015. Adv Nutr. 2016; 7(2): 418-9. doi: 10.3945/an.116.012211, PMID 26980827.
9. Bray F, Ferlay J, Soerjomataram I, Siegel RL, Torre LA, Jemal A. Global cancer statistics 2018: GLOBOCAN estimates of incidence and mortality worldwide for 36 cancers in 185 countries. CA Cancer J Clin. 2018; 68(6): 394-424. doi: 10.3322/caac.21492, PMID 30207593.
10. Byrne FP, Jin S, Paggiola G, Petchey THM, Clark JH, Farmer TJ, *et al.* Tools and techniques for solvent selection: green solvent selection guides. Sustain Chem Processes. 2016; 4(1): 1-24. doi: 10.1186/s40508-016-0051-z.
11. Paralikar P. Biogenic synthesis of silver nanoparticles using leaves extract of *Epiphyllum oxypetalum* and its antibacterial activity. *Austin J.* Biotechnol Bioeng. 2014; 1.
12. Subbaiya R, Shiyamala M, Revathi K, Pushpalatha R, Selvam MM. Biological synthesis of silver nanoparticles from *Nerium indicum* and its antibacterial and antioxidant property. Int J Curr Microbiol Appl Sci. 2014;3(1):83-7.
13. Stuart BH. Polymer analysis. John Wiley and Sons; 2008.
14. Inam F, Peijs T. Reaggregation of carbon nanotubes in two-component epoxy system. J Nanostruct Polym Nanocompos. 2006; 2(3): 87-95.
15. Dröge W. Free radicals in the physiological control of cell function. Physiol Rev. 2002; 82(1): 47-95. doi: 10.1152/physrev.00018.2001, PMID 11773609.
16. Dey P, Chaudhuri D, Chaudhuri TK, Mandal N. Comparative assessment of the antioxidant activity and free radical scavenging potential of different parts of *Nerium indicum*. Int J Phytomed. 2012; 4(1): 54.
17. Hossain R, Rahman MA, Rafi MKJ, Siddique TA, Noman AA, Makki A, *et al.* Pharmacological and ADMET-based pharmacokinetic properties of *Syzygium samarangense* var. parviflorum Leaf extract in *in vitro, in vivo*, and *in silico* models. Not Bot Horti Agrobot Cluj-Napoca. 2020; 48(3): 1155-75. doi: 10.15835/nbha48311986.
18. Namian P, Talebi T, Germi KG, Shabani F. Screening of biological activities (antioxidant, antibacterial, and antitumor) of *Nerium indicum* Leaf and Flower extracts. Vacuum. 2013; 10:(11)378-84.
19. Hussein RA, Mohsin AJ. Trypan blue exclusion assay verifies *in vitro* cytotoxicity of new cis-platinum (II) Complex in Human Cells. Baghdad Sci J. 2019; 16(3): 555-9. doi: 10.21123/bsj.2019.16.3.0555.
20. Upadhyay TK, Trivedi R, Khan F, Al-Keridis LA, Pandey P, Sharangi AB, *et al. In vitro* elucidation of antioxidant, antiproliferative, and apoptotic potential of yeast-derived β-1,3-Glucan particles against cervical cancer cells. Front Oncol. 2022; 12: 942075. doi: 10.3389/fonc.2022.942075, PMID 36059639.
21. Matassov D, Kagan T, Leblanc J, Sikorska M, Zakeri Z. Measurement of apoptosis by DNA fragmentation. Methods Mol Biol. 2004; 282: 1-17. doi: 10.1385/1-59259-812-9 : 001, PMID 15105553.
22. Chazotte B. Labeling lysosomes in live cells with LysoTracker. Cold Spring Harb Protoc. 2011; 2011(2):pdb.prot5571. doi: 10.1101/pdb.prot5571, PMID 21285271.
23. Onodera A, Nishiumi F, Kakiguchi K, Tanaka A, Tanabe N, Honma A, *et al.* Short-term changes in intracellular ROS Localisation After the silver nanoparticles exposure depending on particle size. Toxicol Rep. 2015; 2: 574-9. doi: 10.1016/j.toxrep.2015.03.004, PMID 28962392.
24. Kumara Swamy M, Sudipta KM, Jayanta K, Balasubramanya S. The Green synthesis, characterization, and evaluation of the biological activities of silver nanoparticles synthesized from *Leptadenia reticulata* Leaf extract. Appl Nanosci. 2015; 5(1): 73-81. doi: 10.1007/s13204-014-0293-6.
25. Roy I, Magesh KT, Sathyakumar M, Sivachandran A, Purushothaman D, Aravindhan R. Evaluation of wound healing property of the ethanolic extract of *Glycyrrhiza glabra*

on Vero cell lines using *in vitro* scratch assay test. J Pharm Bioallied Sci. 2023; 15;Suppl 1:S630-5. doi: 10.4103/jpbs.jpbs_61_23, PMID 37654411.

26. Dharmadhas JS, Danaraj J, Packiavathy IASV. Green fabrication of *Nerium oleander*-mediated Silver nanomaterials: synthesis, structural, and stability analysis. BioNanoScience. 2023; 13(3): 1177-83. doi: 10.1007/s12668-023-01148-4.
27. Pierzyńska-Mach A, Janowski PA, Dobrucki JW. Evaluation of acridine orange, LysoTracker red, and quinacrine as fluorescent probes for long-term tracking of acidic vesicles. Cytometry A. 2014; 85(8): 729-37. doi: 10.1002/cyto.a.22495, PMID 24953340.
28. Zhitomirsky B, Farber H, Assaraf YG. LysoTracker and MitoTracker red are transport substrates of P-glycoprotein: implications for anticancer drug design evading multidrug resistance. J Cell Mol Med. 2018; 22(4): 2131-41. doi: 10.1111/jcmm.13485, PMID 29377455.
29. Rahman MM, Dhar PS, Sumaia F, Anika F, Ahmed L, Islam MR, *et al.* Exploring the plant-derived bioactive substances as antidiabetic agent: an extensive review. Biomed Pharmacother. 2022; 152: 113217. doi: 10.1016/j.biopha.2022.113217, PMID 35679719.
30. Bharathi V, Shanthi S. Green synthesis of silver nanoparticles from flower extract of *Nerium oleander* and its characterization. World J Pharm Res. 2017; 6(6): 1410-7. doi: 10.20959/wjpr20176-8456.
31. Danaei M, Dehghankhold M, Ataei S, Hasanzadeh Davarani F, Javanmard R, Dokhani A, *et al.* Impact of particle size and polydispersity index on the clinical applications of lipidic nanocarrier systems. Pharmaceutics. 2018; 10(2): 57. doi: 10.3390/pharmaceutics10020057, PMID 29783687.
32. Sebeia N, Jabli M, Ghith A. Biological synthesis of copper nanoparticles, using *Nerium oleander* leaves extract: characterization and study of their interaction with organic dyes. Inorg Chem Commun. 2019; 105: 36-46. doi: 10.1016/j.inoche.2019.04.023.
33. Bahuguna A, Khan I, Bajpai VK, Kang SC. MTT assay to evaluate the cytotoxic potential of a drug. Bangladesh J Pharmacol. 2017; 12(2): 115-8. doi: 10.3329/bjp.v12i2.30892.
34. Sharma AK, Swami AK, Jangir D, Saran M, Upadhyay TK, Prajapat RK, *et al.* An eco-friendly green synthesis of tungsten nanoparticles from *Moringa oleifera* Lam. and their pharmacological studies. Gazi Med J. 2020; 31(4A). doi: 10.12996/gmj.2020.167.
35. Angelova PR, Abramov AY. Role of mitochondrial ROS in the brain: from physiology to neurodegeneration. FEBS Lett. 2018; 592(5): 692-702. doi: 10.1002/1873-3468.12964, PMID 29292494.
36. Mukherjee N, Gaur R, Shahabuddin S, Chandra P. Recent progress in lysosome-targetable fluorescent BODIPY probes for bioimaging applications. Mater Today Proc. 2022; 62: 7082-7. doi: 10.1016/j.matpr.2022.01.220.
37. Baek A, Son S, Baek YM, Kim DE. KRT8 (keratin 8) attenuates necrotic cell death by facilitating mitochondrial fission-mediated mitophagy through interaction with PLEC (plectin). Autophagy. 2021; 17(12): 3939-56. doi: 10.1080/15548627.2021.1897962, PMID 33783309.
38. Saeed M, Al-Keridis LA, Khattak S, Alshuraym L, Alshammari N, Al-Amrah H, *et al.* Green synthesis of zinc oxide nanoparticles using egg white and coriander root waste: characterization and anti-cancer efficacy in Hela cells. Waste Biomass Valor. 2023: 1-7. doi: 10.1007/s12649-023-02318-x.
39. Khalil MA, El-Shanshoury AERR, Alghamdi MA, Sun J, Ali SS. *Streptomyces catenulae* as a Novel Marine actinobacterium Mediated Silver Nanoparticles: characterization, Biological Activities, and Proposed Mechanism of antibacterial Action. Front Microbiol. 2022; 13: 833154. doi: 10.3389/fmicb.2022.833154, PMID 35572675.
40. Bobadilla AVP, Arévalo J, Sarró E, Byrne HM, Maini PK, Carraro T, *et al. In vitro* cell migration quantification method for scratch assays. J R Soc Interface. 2019;16(151): 20180709. doi: 10.1098/rsif.2018.0709, PMID 30958186.
41. Yu G, Chen L, Hu Y, Yuan Z, Luo Y, Xiong Y. Antitumor effects of baicalein and its mechanism via TGFβ pathway in cervical cancer HeLa cells. Evid Based Complement Alternat Med. 2021;2021: 5527190. doi: 10.1155/2021/5527190, PMID 33777154.

Cite this article: Kini R, Trivedi R, Mujahid MH, Patra P, Alharbi SA, Alshammari FD, Bealy MMB, *et al*. Green Synthesis and Characterization of Silver Nanoparticles from *Nerium indicum* and Investigation of Antioxidant and Anti-Cancerous Potential against Cervical Cancer Cell Line (HeLa). Indian J of Pharmaceutical Education and Research. 2024;58(2):565-78.